GIG Research Institute

JOURNAL OF SUSTAINABLE MINING

Volume 21 | Issue 2 Article 7

2022

Unplanned dilution prediction in open stope mining: developing new design charts using Artificial Neural Network classifier

Author(s) ORCID Identifier:
Sultan Korigov 0000-0002-9932-0180
Amoussou Coffi Adoko 0000-0003-1396-7811
Fhatuwani Sengani 0000-0003-4886-1072

Unplanned dilution prediction in open stope mining: developing new design charts using Artificial Neural Network classifier

Abstract

Minimizing dilution is essential in open stope mine design as excessive unplanned dilution can compromise the operation's profitability. One of the main challenges associated with the empirical dilution graph method used to design open stopes is how to determine the boundary of the dilution zones objectively. Hence, this paper explores the implementation of machine learning classifiers to bridge this gap in the conventional dilution graph method. Stope performance data consisting of the stope dilution (unplanned dilution), the modified stability number, and the hydraulic radius were compiled from a mine located in Kazakhstan. First, the conventional dilution graph methods were used to assess the dilution. Next, a Feed-Forward Neural Network (FFNN) classifier was implemented to predict each level of dilution. Overall, the FFNN results indicated that 97% of the stope surfaces were correctly classified, indicating an excellent classification performance, while the conventional dilution graph method did not show a good performance. In addition, the outputs of the FFNN were used to plot new dilution graphs with a probabilistic interpretation illustrating its practicability. It was concluded that the FFNN-based classifier could be a useful tool for open stope design in underground mines.

Keywords

open stope mining, dilution graph, stope overbreak, neural network classifier

Unplanned Dilution Prediction in Open Stope Mining: Developing New Design Charts Using Artificial Neural Network Classifier

Sultan Korigov [a], Amoussou Coffi Adoko [a,*], Fhatuwani Sengani [b]

[a] Nazarbayev University, School of Mining and Geosciences, Nur-Sultan 010000, Kazakhstan
[b] University of Limpopo, Department of Geology and Mining, South Africa

Abstract

Minimizing dilution is essential in open stope mine design as excessive unplanned dilution can compromise the operation's profitability. One of the main challenges associated with the empirical dilution graph method used to design open stopes is how to determine the boundary of the dilution zones objectively. Hence, this paper explores the implementation of machine learning classifiers to bridge this gap in the conventional dilution graph method. Stope performance data consisting of the stope dilution (unplanned dilution), the modified stability number, and the hydraulic radius were compiled from a mine located in Kazakhstan. First, the conventional dilution graph methods were used to assess the dilution. Next, a Feed-Forward Neural Network (FFNN) classifier was implemented to predict each level of dilution. Overall, the FFNN results indicated that 97% of the stope surfaces were correctly classified, indicating an excellent classification performance, while the conventional dilution graph method did not show a good performance. In addition, the outputs of the FFNN were used to plot new dilution graphs with a probabilistic interpretation illustrating its practicability. It was concluded that the FFNN-based classifier could be a useful tool for open stope design in underground mines.

Keywords: open stope mining, dilution graph, stope overbreak, neural network classifier

1. Introduction

Open stope mining is a common mining method employed in hard rock underground mining in many countries due to several advantages [1,2]. One of the distinctive features of open stope mining is that it is a non-entry mining system, where relatively large excavations (stopes) are created after ore extraction. Appropriate stope dimensions mostly control the stability of the stope surfaces, and, if support of the stope walls is required, cable bolts and backfill are usually used. This method has the capacity of achieving higher productivity with lower exposure to unsafe conditions compared to other underground mining methods. However, unplanned dilution due to the instability, sloughing, caving, or overbreak of the hangingwalls and footwalls can inflict high operational costs, and production delays; it may lead to safety concerns in some cases [1,3,4]. Overbreak is referred to as the unplanned volume of unstable rock, which falls from the stope walls beyond the design shape. Dilution, on the other hand, is the amount of overbreak that is removed from the stope and sent to the processing plant [5]. Dilution can be divided into two categories: planned and unplanned. Usually, the planned dilution is considered unavoidable because the waste rock (with low grade ore) is often mined with ore. This type of dilution is included in planned stope dimensions. On the other hand, unplanned dilution can be avoided or reduced by controlling the wall sloughing and overbreak. Factors influencing the unplanned stope dilution include rock mass structures, in-situ stresses, irregular wall geometry, undercutting walls, blast hole deviation, stope life, and the number of blasts used in the stope extraction [2]. A deeper understanding of how these factors are related to dilution can be useful to estimate the expected amount of overbreak and dilution for adequate production planning and scheduling.

Received 10 January 2021; revised 30 April 2022; accepted 30 April 2022.
Available online 10 August 2022

* Corresponding author at:
E-mail address: amoussou.adoko@nu.edu.kz (A.C. Adoko).

https://doi.org/10.46873/2300-3960.1356

Unplanned dilution can be evaluated using empirical charts and other design tools, such as predictive models and sound engineering judgment. The literature reveals a wide variety of methods capable of assessing open stope dilution within the context of open stope design. These include numerical modelling [3,6–8], analytical methods [9], back analysis of stope monitoring data [10], and empirical dilution graphs [11–13]. Among these methods, the dilution graphs, which were elaborated on the stability graph method [14], are commonly used because of their practical relevance, simplicity, and flexibility [15–17]. The equivalent linear overbreak or slough (ELOS) parameter was introduced to estimate the dilution in the stope walls [5,13]. The ELOS graphs are practical design tools that can be used to select the dimension of the stopes that allow for an acceptable level of dilution.

Nevertheless, these graphs have several drawbacks similar to any other empirical method. They often face the problem of generalization and tend to be overly site-specific. Another challenge with the stability graph approach is how to determine the design lines reliably even though binary classification methods, such as logistic regression techniques, have been used for this purpose [18]. To overcome some of the limitations of the stability graph method, Papaioanou and Suorineni [19] attempted to generalize the dilution graph independent of the ore body size using the Bayesian discrimination method. Nevertheless, the results did not indicate any substantial improvement in prediction and generalization capabilities. These examples clearly demonstrate the urgent need for the improvement of the existing empirical design tools to ensure the profitability and sustainability of the operations, especially in today's mining industry, where most mines tend to go deeper across the world due to the depletion of shallow minerals.

In this regard, the quest for enhancing the open stope design tools has led several researchers to explore alternative tools such as soft computing techniques. For example, Jang et al. [20] proposed a general model for unplanned dilution and ore loss prediction in long-hole stoping mines using a multi-layer Artificial Neural Network (ANN). The correlation coefficient of the proposed model for the three mines involved in their study ranged between 0.66 and 0.72. This fair prediction capability was probably due to the quality and range of the data as they came from various mines, different operating conditions, and where mines were mixed together. Zhao and Niu [15] predicted the ELOS based on four input parameters and multi-layer ANN. Their study showed that better prediction accuracy can be obtained when the model is calibrated to a specific mine site which corroborates the need to consider the site specificity and avoid generalizing in open stope design [21]. However, Zhao and Niu [15] have used a linear activation function in the output layer, which shows that the ELOS model was not a classifier. A few other studies have shown the adequacy and the usefulness of expert systems and decision making algorithms to estimate unplanned dilution. These include a decision support system of unplanned dilution and ore-loss in underground stoping operations using a neuro-fuzzy system [22]; an unplanned dilution index through rating a new classification system for cut-and-fill stoping method [23]; a knowledge-based system for assessing unplanned dilution in open stopes [24]. In addition, ANN can be used to quantify the effect of the parameter contributing to unplanned dilution in underground stoping mines by examining the connection weights of input to hidden layers [16]. More recently, Bazarbay and Adoko [25] illustrated the inadequacy of using ANN as a fitting function for the prediction of the unplanned dilution and suggested that ANN can be used as a classifier. However, the context of their study was limited to a comparative study based on data compiled from various sources.

While the literature indicates a number of studies in which machine learning was used to principally predict the amount of unplanned dilution, as mentioned previously, the implementations of ANN as classifiers to estimate the unplanned dilution levels, however, are surprisingly very limited. Perhaps, many researchers overlook the advantages of simple ANN classifiers due to advancements in soft computing. Yet the majority of rock engineering problems, such as unplanned dilution, should be regarded as classification problems since rock mass classification, and other different forms of ratings and decision makings are involved [26]. Unlike ANN as predictive models, the outputs of ANN classifiers can be conveniently used to plot design charts which are in practice more useful in mine design [11,27]. Therefore, this paper makes use of a multi-layer ANN classifier to establish unplanned dilution graphs that can be employed to design open stopes in underground mines, with the ultimate goal of bridging the gap outlined above and within the scope of the empirical stability graph design approach.

2. Methods

2.1. An overview of the stability graph

The stability graph, also known as Mathew's stability graph, is an open stope design tool that was

proposed by Mathews et al. [14]. The method was initially established on a relatively small number of stope wall stability cases from Canadian mines. Since then it, has been used at various mine sites around the world. Over the past three decades, significant amounts of new data were collected by various researchers, allowing further enhancement of the stability chart [12,18]. As a result, several modifications were made to the method for calculating the governing factors of the stability number, which have led to the establishment of several variants of the stability chart [28].

The stability graph hypothesizes that the competency of the surrounding rock mass could be related to the size of an excavation surface and, therefore, provides an approximation of the critical dimensions of the stopes that will guarantee a desirable design performance (i.e., stability or dilution). It is an empirical graph representing a series of stope surfaces with their corresponding stability conditions. Fig. 1a–b illustrate the stability graph (extended stability graph), and the dilution graph, respectively. In these graphs, a 2-D representation is adopted by plotting the modified stability number N' (or the original stability number N) vs, the Hydraulic Radius (HR). N' is determined according to Eq. (1) as follows:

$$N' = Q'ABC \tag{1}$$

where: A is the rock stress adjustment factor, B is the joint orientation adjustment factor, and C is the gravity adjustment factor. Q' represents the rock mass quality and is defined as per Eq. (2):

$$Q' = \frac{RQD}{J_n}\frac{J_r}{J_a} \tag{2}$$

In Eq. (2), the parameters are the well-known inputs of the Q-system for rock mass classification [29]: RQD, J_n, J_r, and J_a stand for the rock quality designation, joint set number, joint roughness number, and joint alteration number, respectively. The adjustment factors A, B and C in Eq. (1) are determined using design charts [12,18,28]. Factor A reflects the effects of induced stresses on the stope surface; factor B accounts for the joint effect that may cause instability depending on the orientations; and the gravity factor C reflects the mode of failure, which may be in the form of gravity fall, sliding, or slabbing [30].

The variable HR, which reflects the geometry of the stope face, is defined by dividing the area of a stope face over its perimeter (Eq. (3)):

$$HR = \frac{\text{Area}(m^2)}{\text{Perimeter}(m)} \tag{3}$$

2.2. A brief overview of Artificial Neural Network (ANN)-classifiers

An ANN is a form of mathematical representation where processing units known as neurons are interconnected in a way that they are capable to learn from sample data presented to them similar to the human brain's cognitive processes [31]. Their purpose is to "intelligently" recognize any association between data, such as, correlations and patterns. The neurons are compactly interconnected in a configuration that makes large parallel computations possible. An input vector is processed in each neuron n, and the corresponding output is determined according to Eq. (4):

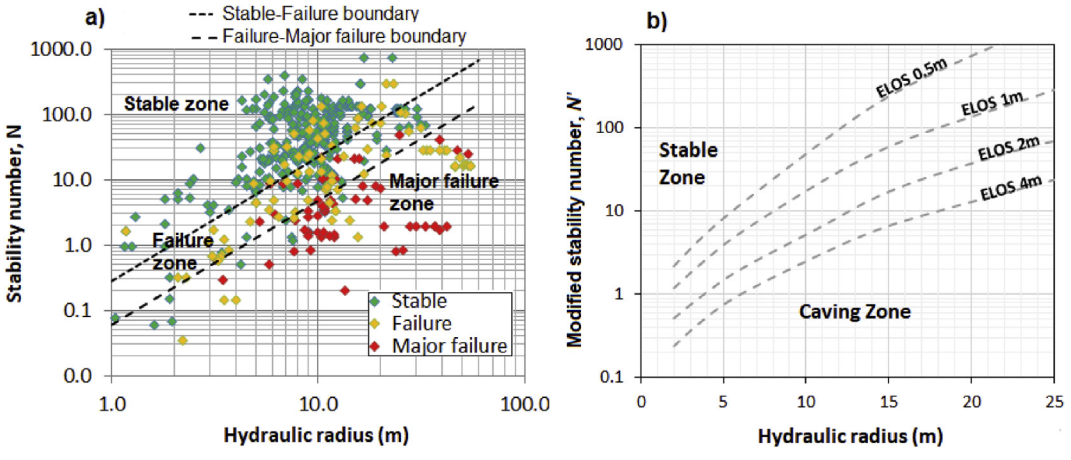

Fig. 1. (a) Stability graph using the extended stability database [18]; (b) Dilution graph showing the stope design lines [5].

$$y = f\left(\sum_{i=1}^{n} w_i x_i + \theta\right) \quad (4)$$

where: x_i, w_i, θ and f are the ith input, ith weight, the bias of the neuron and the activation function of that neuron, respectively [32].

In general, a network comprises a minimum of three layers of processing units (input, hidden, and output layer), as sketched in Fig. 2. The first layer (input layer) only handles the input data without processing. The next layers are known as hidden layers. The last layer denotes the output layer, where the network output is processed, and layers' outputs can be explicitly determined. The network output is computed using initial weights and biases based on a par of dataset (inputs and targets vectors). Subsequently, the weights and biases are adjusted through an algorithm, where the output and the target values are constantly compared until the network outputs meet the targets within an acceptable error. Typically, the acceptable error indicator is the sum of squared errors, which are minimized through learning algorithms, such as the Levenberg-Marquardt algorithm. In the network structure, several types of ANNs can be employed, including back-propagation, counter-propagation, feedforward, and dynamic networks. Depending on the network structure, they can be used to solve different kinds of problems, such as data fitting, pattern recognition, classification, clustering, and time series [33]. When ANNs are employed as a classifier, several network configurations can be used in accordance with the data patterns to classify the parameter under consideration (e.g., stope dilution). For instance, commonly used classifiers

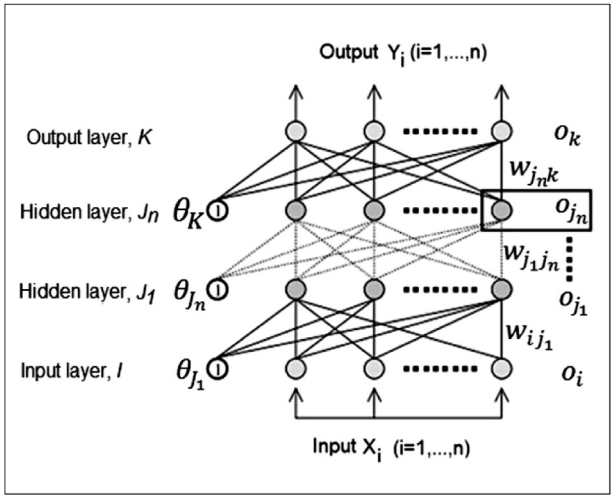

Fig. 2. A feed-forward neural network schematic diagram.

are the one-against-all, weighted one-against-all, binary-coded, parallel-structured, weighted parallel-structured, and tree-structured [34].

2.3. Data description

For this study, stope dilution data were collected from the Ridder-Sokolny mine, located in East Kazakhstan. Owned by Kazzinc Corporation, the mine currently produces 1.6 million tons of ore annually with an average gold grade of 2.0 g/ton [35]. A number of mining methods are utilized at the Ridder-Sokolny mine depending on the ore body morphology and thickness, such as sublevel caving, cut-and-fill stoping, and sublevel stoping. The rock mass quality of the area of study varies from poor to very good. The compiled data consists of the rock mass properties (e.g., *RQD*, joint set number J_n, joint roughness coefficient J_r, joint alteration number J_a), stope geometry, and the stope reconciliation data. This allowed determining the modified stability number (N'), hydraulic radius (*HR*), and the overbreak percentage. All N' and *HR* values were determined from mine plans and final stope shapes from stope surveying data (cavity monitoring surveying, CMS), mining plans, and geotechnical reports. The stope overbreak and dilution were determined using comparison between the initially designed stope sizes with the final resultant stope sizes, and were measured by CMS with the aid of a mine design software, Datamine Studio RM®.

The database contains 147 case histories of stope walls. The N' values range from 10.8 to 46.4, and the *HR* values vary from 1.7 to 12.3 m. The same dilution data (147 data points in total)used previously were categorized into three groups: minor dilution, moderate dilution, and major dilution according to the percentage of overbreak. Thresholds of 20 and 50% overbreak were used for this purpose based on the acceptable dilution in the Ridder-Sokolny mine and the requirement to keep statistical consistency of the data. This led to 60, 44, and 43 cases of minor (less than 20% overbreak), moderate (between 20 and 50%), and major (more than 50%) cases of dilution, respectively. A distribution (pair plot) of the dataset is shown in Fig. 3, while the coefficients of correlation of the dilution parameters are summarized in Table 1, where weak linear correlations can be seen. Fig. 3 represents pairwise relationships of the main variables in the dataset, i.e. dilution, *HR* and N'. On the diagonal, a univariate distribution plot is given to highlight the marginal distribution of each of these variables.

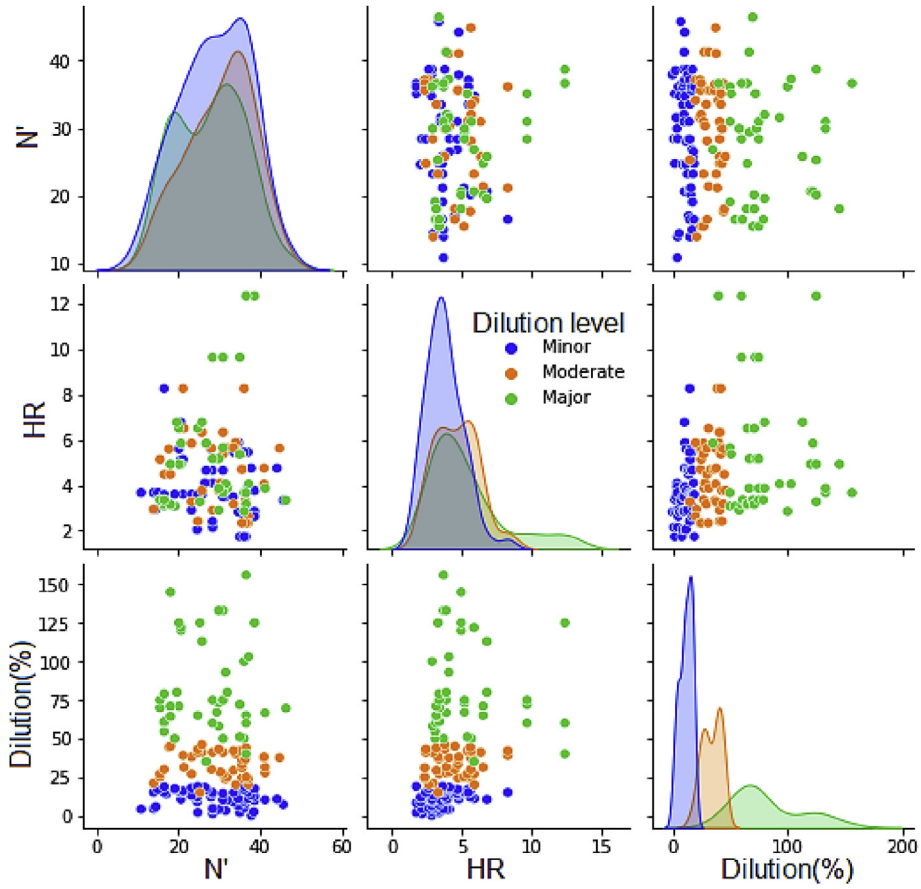

Fig. 3. Pair plot of the main variables of the data used in the study.

3. Results

3.1. The stability graph

In this section, the stability graphs are plotted using the compiled database following the methodological procedure described in Section 2.1 for a qualitative assessment of dilution. In Fig. 4a, the data points of the current study were superimposed on the stability graph in use in the Ridder-Sokolny mine, where the boundaries between stable and caved zones were roughly established based on engineering judgement. In Fig. 4b the data points were superimposed on the extended stability graph; the boundaries of the zones were determined objectively using logistic regression [18]. It can be seen from these graphs that almost all of the data points fall within the stable zone. This means dilution is unlikely to be linked to stope wall instability and sloughing. Next, the quantitative stability graph or ELOS graph [5,13] corresponding to the dilution database was produced, as shown in Fig. 4c. The graph shows that the expected dilution is less than 0.5 m. On the other hand, higher dilution levels were observed in the database (see Fig. 4). The observed stopes had been experiencing unplanned dilution at varying rates; meanwhile, the stability graph-based dilution graphs predicted very limited dilution. Therefore, it is deduced that ELOS methods together with Mathew's stability graphs are not good predictors of unplanned dilution in the Ridder-Sokolny mine. Thus, it becomes necessary to explore other ways of predicting unplanned dilution.

Table 1. The correlation coefficients of the dilution parameters.

Parameters	N'	*HR*	Dilution (%)
N'	1		
HR	0.05	1	1
Dilution (%)	−0.07	0.27	1

3.2. Establishing the ANN-classifier

3.2.1. Input data description and network optimization

The ANN-classifier is developed on the basis of the same dilution data (147 data points in total) used in Section 3.1. Matlab software was used for the

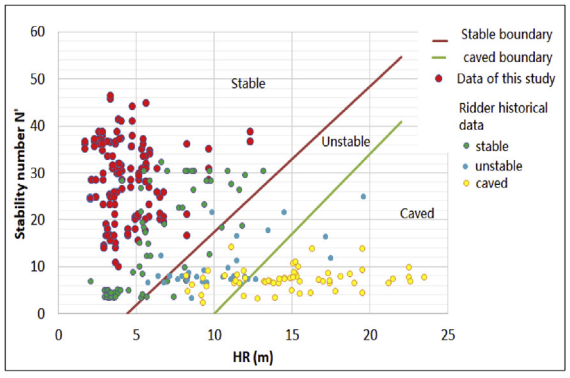

a)

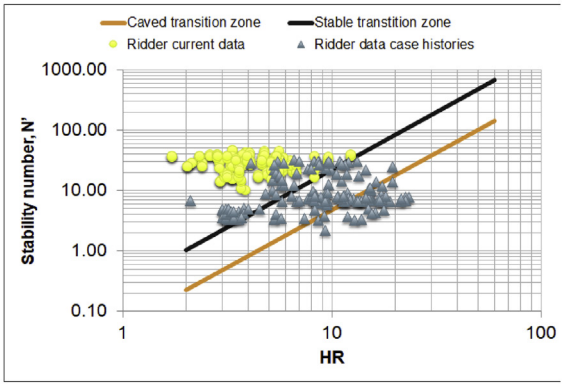

b)

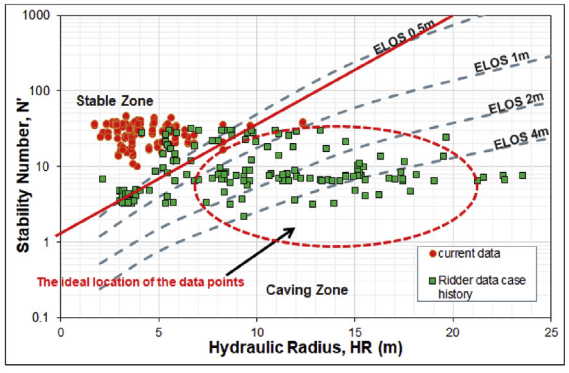

c)

Fig. 4. (a) Ridder-Sokolny data points on Mathews' stability graph; (b) Ridder-Sokolny data points on the extended stability graph; (c) Ridder-Sokolny data points superimposed on the ELOS graph.

computation. The input parameters for the neural network are stope geometry, defined by the hydraulic radius (*HR*), and the rock mass characteristics, represented by the Modified Stability Number (N'). The target is the overbreak category, which also represents the level of dilution. The data were randomly split into three groups: training (70%), validation (15%), and testing (15%) datasets. These datasets sizes were found adequate for the modelling [31]. The target is represented by specific vectors as follows: (1, 0, 0); (0, 1, 0); and (0, 0, 1), which represent minor, moderate, and major overbreak, respectively. These vectors are applied to satisfy the conditions of having the $n \times n$ identify matrix (n is the number of classes) representing the targets in pattern recognition networks. A series of experiments were conducted using a trial-and-error principle until the optimum network was found. The best performance was obtained for a two-hidden layers feed-forward neural network (FFNN), which was found to be the optimum network in the experiments. The hidden layers have 102 neurons each. The performance of the network was evaluated using the cross-entropy algorithm. This algorithm determines the network performance constrained by the targets, outputs, and performance weights with a measure that heavily penalizes extremely inaccurate outputs, i.e., when targets and outputs are too far from each other. Conversely, a very little penalty is considered for fairly correct classifications. Therefore, reaching a minimum cross-entropy error leads to good classifiers. Fig. 5 displays the performance of the optimum network configuration with respect to the validation dataset. The cross-entropy error reached a minimum value of 0.0759 at epoch 21 (an epoch represents a completed iteration or cycle of the training procedure). The activation functions, which were used, included the logistic sigmoid (Logsig) function in the hidden layers and the *softmax* function in the output layer. They are defined according to Eqs. (5) and (6):

$$\log sig(n) = \frac{1}{1+e^{-n}} \tag{5}$$

$$soft\ \max(n) = \frac{e^n}{\sum e^n} \tag{6}$$

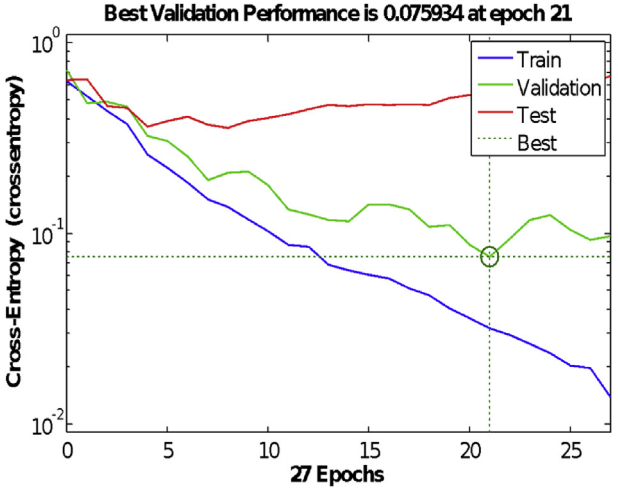

Fig. 5. The validation performance (error) graph.

Eq. (6) indicates that the output values not only fall within the internal [0,1] but also sum to 1, allowing probabilistic interpretation. The *softmax* activation function is often used in the output layer of a neural network with the purpose of normalizing the output of a network to a probability distribution over predicted output classes. Hence, the outputs of the FFNN can be considered as the probabilities of occurrence of stope walls with minor, moderate, and major dilution in the classification.

3.2.2. Classification results

The confusion matrix representing the dilution classification is shown in Fig. 6. It reflects the predictive performance of the classifiers. This matrix compares the results simulated by the model with identified target values. On the diagonal, the correctly predicted values are shown (green cells). In total, 143 cases out of 147 were correctly predicted. Only four cases were misclassified. The confusion values (shown in the blue cells) indicate the degree of misclassification. The closer to zero is the confusion value, the better the classification. Based on the data collected from the Ridder-Sokolny mine, the confusion values for training, validation, testing, and all datasets together are 0.0, 4.5, 13.6, and 2.7%, respectively, which indicate a high degree of accuracy. This classification performance is extremely good. Based on the testing data, the interpretation of these results (considering the worst-case scenario) is that if 100 new stope surfaces from the Ridder mine were to be evaluated by the proposed FFNN, only 14 stope surfaces would likely be misclassified. . This performance is very good compared to the stability graph-based dilution ELOS as shown in Section 3.1.

3.2.3. Classification performance

The Receiver Operating Characteristics (ROC) was used to check the quality of the classification. The ROC charts are plotted in Fig. 7. The ROC uses a specific value of the output (threshold) to identify each dilution class [36]. The true positive and true negative rates are calculated and plotted on the

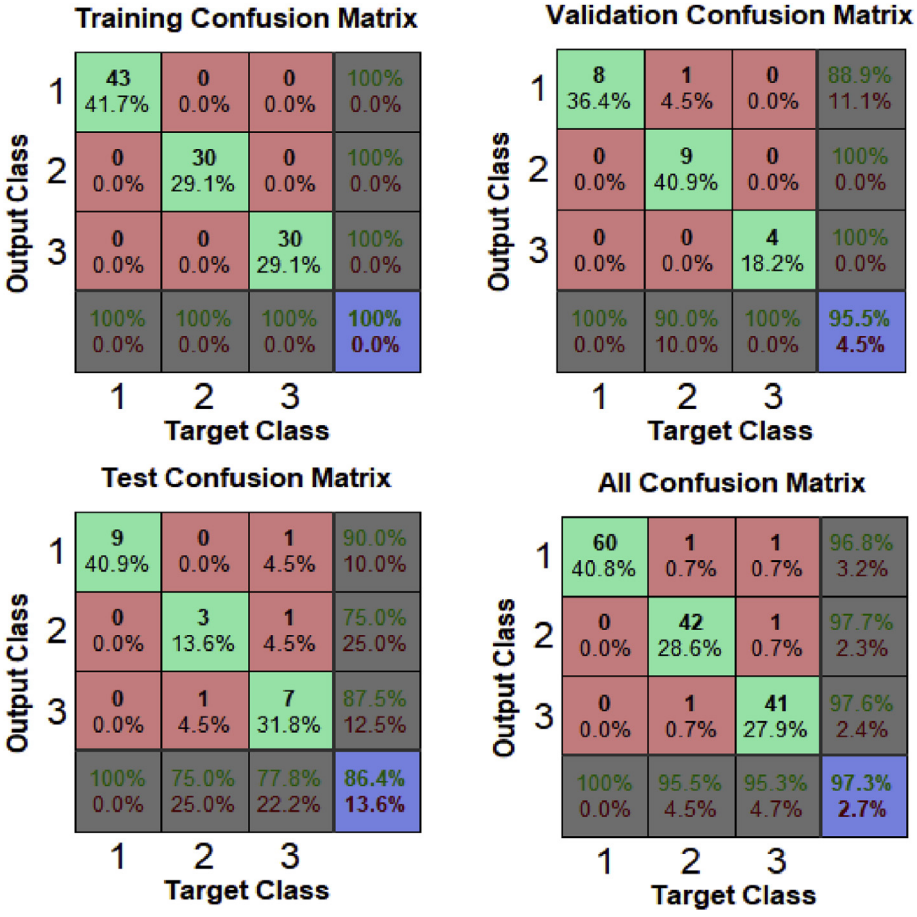

Fig. 6. Confusion matrix for the datasets.

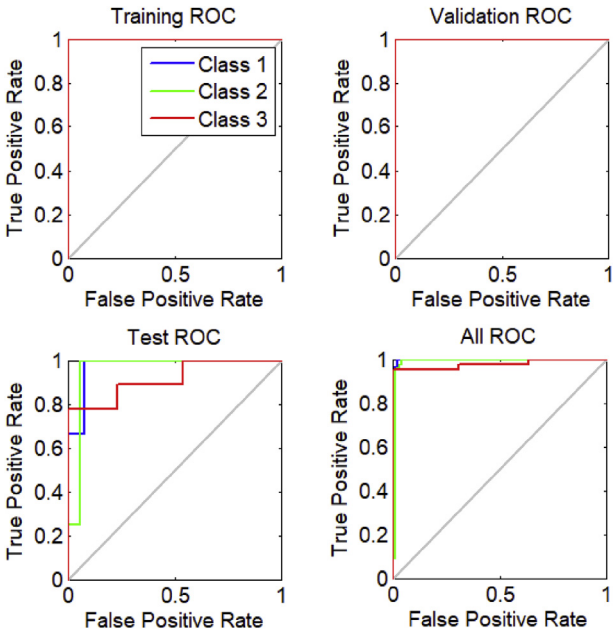

Fig. 7. ROC diagrams showing the classification performance.

graph. The ROC curves indicate a better classification when they get closer to the left upper corner of the diagram [37]. When the curve reaches the diagonal line in the plot, it indicates a poor classification. For each dataset (training, testing, validation, and whole data), it can be seen that all classes are classified well, and all curves are located in the upper left corner. This is in good agreement with the confusion matrix.

Furthermore, the performance of the classification was assessed based on the entire dataset through the performance indices defined in Eqs. (7)–(9), namely, the accuracy, sensitivity and specificity:

$$\text{Accuracy} = \frac{T_p + T_n}{T_p + T_n + F_p + F_n} \tag{7}$$

$$\text{Sensitivity} = \frac{T_p}{T_p + F_n} \tag{8}$$

$$\text{Specificity} = \frac{T_n}{T_n + F_p} \tag{9}$$

where: T_p, T_n, F_p and F_n represent the true positive, true negative, false positive, and false negative, respectively. The computed indices are summarized in Table 2.

As shown in Table 2, the average accuracy of the classification is 98%, which indicates that the proposed ANN classifier has excellent prediction capability.

Table 2. Summary of the classification performance.

Dilution level	Accuracy	Sensitivity	Specificity
Minor dilution (<20% overbreak)	0.99	1.00	0.98
Moderate dilution (20–50% overbreak)	0.98	0.95	0.99
Major dilution (>50% overbreak)	0.98	0.95	0.99
Average	0.98	0.97	0.99

3.2.4. Probabilistic dilution graph plots

The network output values were used to plot the ANN-based dilution graphs. A sample of the computed output is provided in Table 3. This output is a vector representing minor, moderate, or major dilution according to the largest value of its component. For example, the vector (0.0004, 0,9923, 0.0073) highlighted in bold and shown in Table 3, defines a moderate case of dilution.

The probability of each dilution category is illustrated in Fig. 8a-d. They provide a visualization of dilution areas with their corresponding probability. These areas are displayed by probability color code indicating the zone of minor, moderate, or major dilution. The minor dilution (Fig. 8a) is plotted on the stability graph, where N' and HR relationship is shown. Yellow-colored zones show the highest probability of the stope with minor dilution, while the lowest probability of a particular dilution category is colored in red. From Fig. 8a, the minor dilution with a probability of more than 0.9 corresponds to a zone with $HR > 7$ and $N' < 15$, while for the HR less than 7, minor dilution is likely to occur regardless of the stability number (N''). It is noted that in the range of HR between 5 and 7, an erratic outcome is observed. Here, the presence of moderate and major dilution can be observed as the probability of minor dilution drastically changes. In addition, with high values of HR ($HR > 7$) and low stability number ($N' < 20$), minor dilution is likely to occur without high ore contamination. Compared with the conventional dilution graphs, this graph reflects more details and provides additional information, i.e., the dilution level's probability. The interpretation of the ANN-based dilution graph is more straightforward. However, from Fig. 8a–c, it can also be seen that the stability number (N') is not a good predictor of dilution.

In Fig. 8a-b moderate and major dilution graphs are illustrated respectively. Similar to Fig. 8a, a probability code, yellow and green colored zone indicate potential zones of moderate dilution. Based on Fig. 8c showing the probabilities of occurrence of the major dilution class, a zone with high HR and N' and a zone with low hydraulic radius and low

Table 3. Selected computed data of dilution categories classification.

Input		Overbreak (%)	Dilution level	Target (vector)			Output (vector)		
HR (m)	N′								
9.64	28.36	60.00	Major	0	0	1	0.0000	0.0008	0.9992
2.15	28.40	1.20	Minor	1	0	0	0.9995	0.0005	0.0000
8.26	36.09	42.00	Moderate	0	1	0	**0.0004**	**0.9923**	**0.0073**
3.87	31.96	80.00	Major	0	0	1	0.0000	0.0007	0.9993
3.94	37.12	11.00	Minor	1	0	0	0.9988	0.0012	0.0000
4.76	41.02	38.04	Moderate	0	1	0	0.0003	0.9985	0.0011
3.36	15.47	75.00	Major	0	0	1	0.0000	0.0005	0.9995
4.93	20.62	120.00	Major	0	0	1	0.0000	0.0002	0.9998
3.94	29.90	4.00	Minor	1	0	0	0.9996	0.0004	0.0000
2.05	24.61	8.90	Minor	1	0	0	0.9992	0.0008	0.0000
3.28	25.26	44.00	Moderate	0	1	0	0.9983	0.0017	0.0000
2.94	13.92	21.00	Moderate	0	1	0	0.0978	0.9019	0.0003
2.33	37.12	24.00	Moderate	0	1	0	0.0048	0.9949	0.0004
5.59	28.00	12.00	Minor	1	0	0	0.9993	0.0007	0.0000
5.63	28.08	30.00	Moderate	0	1	0	0.0006	0.9992	0.0002
9.64	30.93	75.00	Major	0	0	1	0.0000	0.0003	0.9997

stability number (colored yellow) show to have a high dilution of more than 50%. Major dilution points can also be located in the stable and transition zones of the conventional stability graph. In Fig. 8d, the probability distribution of minor dilution is represented on a 3D graph. The highest probability of dilution prevails in the red color red, while the lowest probability is in blue. This map allows visualization of how dilution changes in three dimensions. The probability map from Fig. 8d provides an advantage of visualizing dilution at different points. Minor dilution has a low probability of occurrence in the stable zone. Occasionally, no strong dependency of hydraulic radius influence

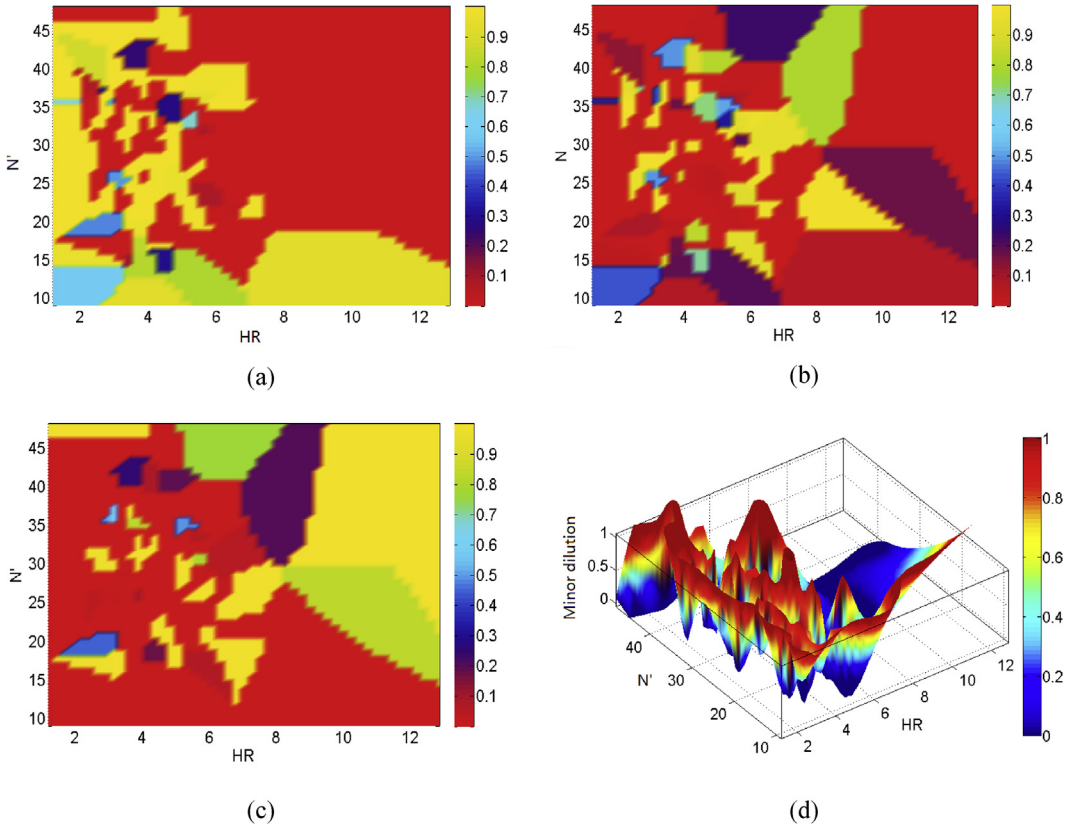

Fig. 8. Probabilistic dilution graphs: (a) Minor dilution; (b) Moderate dilution; (c) Major dilution; (d) 3D minor dilution map.

on the minor dilution is observed. In the stable zone, moderate and major dilutions also exist. Similar maps can be plotted for moderate and major dilution cases.

4. Discussions

The stability graph approach was used to evaluate unplanned stope dilution associated with data obtained from the Ridder-Sokolny mine and the results indicated low dilution levels. However, the actual recorded dilution level from the mine stope reconciliations showed high dilution. These results clearly demonstrated that the stability graph method is not always adequate for predicting the dilution level. This led to investigating an alternative method that could accurately classify and predict the dilution of stope more consistently through ANN-based dilution graphs.

As shown in section 4.2.3, the ANN classifier model indicated very good classification performance, 98% of accuracy on average. These results outperform many of the existing ones, as shown in Table 4. In that table, two different performance indices were used. Even though they have different meanings, they can be used to evaluate the performance of the ANN model. R is the coefficient of correlation between predicted dilution and actual dilution, which indicate the fitness of the model while in the classifier models, the accuracy is calculated using Eq. (7). Based on Table 4, the performance of our model is similar to that of Zhao and Niu [15]. In both studies, the data came from a single mine, and high accuracy was obtained, which confirms the site specificity of the ANN model. Nevertheless, these models are valid for values of the input parameters within the data range i.e., the minimum and maximum values.

Another contribution of this study is its performance over other classification methods. Taking into consideration a few well known works related to the use of the stability graphs either qualitatively or quantitatively with different databases across the world, the percentage of the stope performance cases correctly classified (classification accuracy or sensitivity, and discriminability index) commonly range from 23 to 88%, depending on the source of the data [18,19,38,39]. In these works, statistical tools, such as logistic regression and Bayesian discrimination, were employed to objectively classify the stope performance data into categorical responses according to some design lines. Yet, very high misclassification was observed [19]. In the current study, there is no need for the use of such design lines as seen in these previous studies. The absence of these lines contributed to the improvement of classification accuracy.

The relatively poor to fair accuracy in existing works is because the method was initially developed as a non-rigorous method, and a series of simplifications and assumptions were considered [30]. Several limitations of the stability graph method have already been highlighted in previous studies [4,40]. For example, the sliding failure modes in footwalls, the instabilities caused by tension, complex stope geometries, poor blasting effects, stand-up time, the effect of nearby faults, and subjectivities in defining the stability graph zones, etc., have not been taken into consideration in the stability graph. Nevertheless, it is evident that incorporating the effects of each of these factors into the stability graph is a daunting task; this would even defeat the purpose of the method itself, which is its simplicity. On the other hand, the ANN-based graph method can incorporate all these effects in the development of the classifier. For example, although

Table 4. Performance comparison summary of related study.

References	Methods	Accuracy
Jang et al. [22]	Concurrent neuro-fuzzy system; data size = 1067 cases; input parameters include stope geometry, blasting and geology	$R = 0.719$
Jang et al. [20]	ANN with one hidden layer; data size = 1067 cases; input parameters include stope geometry, blasting and geology	$R = 0.66–0.72$
Zhao and Niu [15]	Multi-layer ANN; data size = 120 cases; input parameters include stope geometry, blasting and rock mass properties	$R = 0.98$
Mohseni et al. [23]	Expert system based on Fuzzy-Delphi analytical hierarchy process; Data size = 10 case histories; input parameters include stope geometry, drilling & blasting, geology and operational parameters	$R = 0.94$
Bazarbay and Adoko [25]	ANN classifier; data size = 227 cases; input parameters include stope geometry and the stability number	85% using Eq. (7)
Bazarbay and Adoko [24]	Fuzzy inference system; data size = 147 cases; input parameters include stope geometry and the stability number	84% using Eq. (7)
This study	ANN classifier; data size = 147 cases; input parameters include stope geometry and the stability number	98% using Eq. (7)

not provided in this study, an exploratory model of the classifier was considered, where the stope dimensions, the in-situ stress, stope wall orientations, discontinuity characteristics, and the rock mass properties were directly used without calculating *HR* and *N′*. In that model, the overall misclassification rate (4%) was close to that of this study (2.7%). This means with this method, many more influencing factors could be considered in the modelling. In addition, calculating the stability number can then be omitted, which eliminates the unnecessary debate about whether the stability number (N) or the modified stability number (N'') should be used in the stability graph method, as presented in a recent study [41]. Furthermore, the results of the present study also demonstrate that for the database used in this study, the stability number is not a good predictor of dilution, and the dilution graph cannot be generalized as the dilution seems to be associated with certain values of *HR*, which are being dictated by the mean ore width. It is worth mentioning that although the method appeared to be useful and relevant to the study area, an extensive database (i.e., sufficiently large data with higher variability) of various stopes with different geometry and rock mass properties is still required for further validation of the method proposed in this study. This will increase the data range, minimize the influence of subjective data, and ultimately enhance the generalization of the classifiers. When new data become available, the probability maps will be updated, and the method will be continuously improved.

5. Conclusions

In this paper, a new dilution graph is proposed. It was developed based on a feed-forward ANN classifier consisting of two hidden layers. Unplanned dilution data collected from the Ridder-Sokolny mine were used to train, test, and validate the classifier. The main parameters included the modified stability number, hydraulic radius, and the stope overbreak. The level of dilution was categorized into three classes: minor, moderate, and major dilution, based on stope overbreak. Overall, 97% of the stope surfaces were correctly classified. These results show higher predictor capability compared with those of the conventional stability graph. More than 97% of the stope dilution data were properly classified. On the other hand, the results of the conventional stability graph method showed inconsistency in assessing the level of dilution in the Ridder-Sokolny mine. The stopes observed had been experiencing unplanned dilution at varying rates, while the stability-based dilution graphs predicted very limited dilution. This justified the implementation of the non-conventional ANN-based dilution graph. It was found that the ANN-classifier showed merits in assessing the dilution level. Furthermore, the network output values were found to be useful in plotting the probabilistic dilution maps, which are convenient for stope design and less experienced users of the conventional stability graph charts. This allows for the selection of the dimension of the stopes that would correspond to the acceptable dilution level in a probabilistic sense. It was concluded that the ANN-based dilution graph would be a good tool for dilution evaluation in the Ridder-Sokolny mine (or any mine with the same data range).

However, more data (i.e., increasing the data range) is needed to generalize the methodology as this study relies on site-specific data. Care must be taken not to advance overconfidence in a result without recognizing the nature of the information underlying the strategy. Hence, it is suggested to increase the size and quality of the dilution database to increase the method's generalization capability. The merit of this study lies in the implementation of an ANN-based classifier to produce probability contours for the level of dilution highlighted and color-coded. There is no need to use any zone delineation for the dilution, as commonly seen in the conventional method. The graphs provide a probabilistic interpretation of the stope dilution, where the uncertainties inherent in the stope design can be straightforwardly quantified. This would make the ANN-based classifier a convenient tool for risk assessment and the optimization of the open-stope design.

Conflicts of interest

The authors declare no conflict of interest.

Ethical statement

The authors state that the research was conducted according to ethical standards.

Funding body

This research was funded by Nazarbayev University, grant number 090118FD5338.

Acknowledgments

The authors would like to acknowledge the contribution of the authorities of the Ridder-Sokolny mine for providing access to their mine and relevant data for this study.

References

[1] Pakalnis RT, Poulin R, Hadjigeorgiou J. Quantifying the cost of dilution in underground mines. Min Eng 1995;47:1136–41.
[2] Potvin Y, Hudyma M. Open stope mining in Canada. In: MassMin 2000. Brisbane, Queensland, Australia: Australasian Institute of Mining and Metallurgy; 2000.
[3] Henning JG, Mitri HS. Numerical modelling of ore dilution in blasthole stoping. Int J Rock Mech Min Sci 2007;44: 692–703.
[4] Adoko AC, Yakubov K, Alipov A. Mine stope performance assessment in unfavorable rock mass conditions using neural network-based classifiers. In: YSRM2019 & REIF2019. Okinawa, Japan: ISRM & The Japanese Society for Rock Mechanics; 2019.
[5] Capes GW. Open stope hangingwall design based on general and detailed data collection in rock masses with unfavourable hangingwall conditions. Ann Arbor: The University of Saskatchewan; 2009. p. 301 (Canada).
[6] Wang J, Milne D, Wegner L, Reeves M. Numerical evaluation of the effects of stress and excavation surface geometry on the zone of relaxation around open stope hanging walls. Int J Rock Mech Min Sci 2007;44:289–98.
[7] El Mouhabbis HZ. Effect of stope construction parameters on ore dilution in narrow vein mining. In: Department of mining and materials engineering. Montreal, Canada: McGill University; 2013.
[8] Heidarzadeh S, Saeidi A, Rouleau A. Use of probabilistic numerical modeling to evaluate the effect of geomechanical parameter variability on the probability of open-stope failure: a case study of the niobec mine. Quebec (Canada): Rock Mechanics and Rock Engineering; 2019.
[9] Diederichs MS, Kaiser PK. Tensile strength and abutment relaxation as failure control mechanisms in underground excavations. Int J Rock Mech Min Sci 1999;36:69–96.
[10] Cepuritis PM, Villaescusa E, Beck DA, Varden R. Back analysis of over-break in a longhole open stope operation using non-linear elasto-plastic numerical modelling. In: 44th U.S. Rock mechanics symposium and 5th U.S.-Canada rock mechanics symposium. Salt Lake City, Utah: American Rock Mechanics Association; 2010. p. 11.
[11] Pakalnis R. Empirical design methods in practice. In: Potvin Y, editor. Proceedings of the international seminar on design methods in underground mining. Perth: Australian Centre for Geomechanics; 2015. p. 37–56.
[12] Potvin Y. Empirical open stope design in Canada. The University of British Columbia; 1988.
[13] Clark LM. Minimizing dilution in open stope mining with a focus on stope design and narrow vein longhole blasting. In: Mining engineering. Vancouver: University of British Columbia; 1998.
[14] Mathews K, Hoek E, Wyllie D, Stewart S. Prediction of stable excavation spans at depths below 1000m in hard rock mines *CANMET Report, DSS Serial No. OSQ80-00081*. 1981.
[15] Zhao X, Niu J a. Method of predicting ore dilution based on a neural network and its application. Sustainability 2020;12.
[16] Jang H, Topal E, Kawamura Y. Illumination of parameter contributions on uneven break phenomenon in underground stoping mines. Int J Min Sci Technol 2016;26: 1095–100.
[17] Zhalel M, Adoko AC, Korigov S. An approach to stope stability assessment in open stope mining environment. In: *54th U.S. Rock mechanics/geomechanics symposium,* (physical event cancelled: American rock mechanics association; 2020. p. 6.
[18] Mawdesley C, Trueman R, Whiten WJ. Extending the Mathews stability graph for open–stope design. Min Technol 2001;110:27–39.
[19] Papaioanou A, Suorineni FT. Development of a generalised dilution-based stability graph for open stope design. Min Technol 2016;125:121–8.
[20] Jang H, Topal E, Kawamura Y. Unplanned dilution and ore loss prediction in longhole stoping mines via multiple regression and artificial neural network analyses. J S Afr Inst Min Metall 2015;115:449–56.
[21] Stewart PC, Trueman R. Strategies for minimising and predicting dilution in narrow vein mines – the narrow vein dilution method. In: Narrow vein mining conference 2008. Ballarat, Australia: Australasian Institute of Mining and Metallurgy; 2008.
[22] Jang H, Topal E, Kawamura Y. Decision support system of unplanned dilution and ore-loss in underground stoping operations using a neuro-fuzzy system. Appl Soft Comput 2015;32:1–12.
[23] Mohseni M, Ataei M, Khaloo Kakaie R. A new classification system for evaluation and prediction of unplanned dilution in cut-and-fill stoping method. J Mining Environ 2018;9: 873–92.
[24] Bazarbay B, Adoko AC. Development of a knowledge-based system for assessing unplanned dilution in open stopes IOP Conference Series. Earth Environ Sci 2021;861:062086.
[25] Bazarbay B, Adoko AC. A comparison of prediction and classification models of unplanned stope dilution in open stope design. In: 55th U.S. Rock mechanics/geomechanics symposium; 2021.
[26] Qi C, Fourie A, Zhao X. Back-analysis method for stope displacements using gradient-boosted regression tree and firefly algorithm. J Comput Civ Eng 2018;32:10.
[27] Wang J, Milne D, Pakalnis R. Application of a neural network in the empirical design of underground excavation spans. Min Technol 2002;111:73–81.
[28] Vallejos JA, Delonca A, Fuenzalida J, Burgos L. Statistical analysis of the stability number adjustment factors and implications for underground mine design. Int J Rock Mech Min Sci 2016;87:104–12.
[29] Barton N, Lien R, Lunde J. Engineering classification of rock masses for the design of tunnel support. Publikasjon - Norges Geotekniske Institutt; 1974.
[30] Stewart SBV, Forsyth WW. The Mathews method for open stope design. Cim Bull 1995;88:45–53.
[31] Adoko AC, Vallejos J, Trueman R. Stability assessment of underground mine stopes subjected to stress relaxation. Min Technol: Trans Inst Min Metall 2020;129:30–9.
[32] Veelenturf LPJ. Analysis and applications of artificial neural networks. Midsomer Norton: Prentice Hall International (UK) Ltd; 1995.
[33] Demuth H, Beale M. Neural network toolbox for use with MATLAB. MA, USA: The MathWorks, Inc.; 2002.
[34] Fausett LV. Fundamentals neural networks: architecture, algorithms, and applications. Englewood Cliffs, New Jersey: Prentice-Hall, Inc; 1994.
[35] KAZZINC 2019 Ridder-Sokolny mine operation. https://www.kazzinc.com/eng/.
[36] Qi C, Fourie A, Du X, Tang X. Prediction of open stope hangingwall stability using random forests. Nat Hazards 2018;92:1179–97.
[37] Adoko AC, Vallejos J, Trueman R. Stability assessment of underground mine stopes subjected to stress relaxation. Min Technol 2020;129:30–9.
[38] Suorineni FT, Kaiser PK, Tannant DD. Likelihood statistic for interpretation of the stability graph for open stope design. Int J Rock Mech Min Sci 2001;38:735–44.
[39] Stewart PC. Minimising dilution in narrow vein mines. In: Julius Kruttschnitt mineral research centre. Queensland: The University of Queensland; 2005.
[40] Suorineni FT. The stability graph after three decades in use: experiences and the way forward. Int J Min Reclamat Environ 2010;24:307–39.
[41] Madenova Y, Suorineni FT. On the question of original versus modified stability graph factors – a critical evaluation. Min Technol 2020;129:40–52.